Energy Conversion and Management 267 (2022) 115866

Contents lists available at ScienceDirect

Energy Conversion and Management

journal homepage: www.elsevier.com/locate/enconman

Life cycle assessment of power-to-methane systems with CO_2 supplied by the chemical looping combustion of biomass

Alberto Navajas [a,b], Teresa Mendiara [c,*], Luis M. Gandía [a,b], Alberto Abad [c], Francisco García-Labiano [c], Luis F. de Diego [c]

[a] Department of Science, Public University of Navarre, Arrosadía Campus s/n, E-31006 Pamplona, Spain
[b] Institute for Advanced Materials and Mathematics (InaMat2), Public University of Navarre, Arrosadía Campus s/n, E-31006 Pamplona, Spain
[c] Department of Energy and Environment, Instituto de Carboquímica-ICB-CSIC, Miguel Luesma Castán 4, 50018 Zaragoza, Spain

ARTICLE INFO

Keywords:
Power-to-methane
Carbon capture
Biomass
Chemical looping
CLOU
iG-CLC

ABSTRACT

Power-to-methane (PtM) systems may allow fluctuations in the renewable energy supply to be smoothed out by storing surplus energy in the form of methane. These systems work by combining the hydrogen produced by electrolysis with carbon dioxide from different sources to produce methane via the Sabatier reaction.

The present work studies PtM systems based on the CO_2 supplied by the chemical looping combustion (CLC) of biomass (PtM-bioCLC). Life- cycle- assessment (LCA) was performed on PtM-bioCLC systems to evaluate their environmental impact with respect to a specific reference case. The proposed configurations have the potential to reduce the value of the global warming potential (GWP) climate change indicator to the lowest values reported in the literature to date. Moreover, the possibility of effectively removing CO_2 from the atmosphere through the concept of CO_2 negative emissions was also assessed. In addition to GWP, as many as 16 LCA indicators were also evaluated and their values for the studied PtM-bioCLC systems were found to be similar to those of the reference case considered or even significantly lower in such categories as resource use-depletion, ozone depletion, human health, acidification potential and eutrophication. The results obtained highlight the potential of these newly proposed PtM schemes.

1. Introduction

The European Union (EU) has set the target of achieving carbon neutrality by 2050, thus paving the way towards the decarbonisation required by the blocs energy system in order to comply with the Paris agreement [1]. Fulfilling this ambition will require wider penetration of renewable energies in the coming decades, which will have to rise from 15% of total primary energy supply (TPES) to 65% by 2050 [2]. In this scenario, long-term energy storage will be crucial if grid security is to be improved by smoothing out the supply fluctuations at times when surplus renewable energy is generated, thus ensuring that generated energy can be discharged and not lost. In fact, the deployment of electricity storage is key if renewable technologies are to reach their expected level of development. It is estimated that electricity storage will account for up to 8% of the overall power capacity installed by 2050 [3], making it necessary to boost the development of storage technologies with low energy costs and high discharge rates. There are four main electricity storage technologies currently being considered: electrical (superconducting magnetic energy storage), mechanical (pumped storage, compressed air, flywheels), thermal (latent heat, sensible heat, thermochemical) and chemical (supercapacitors, batteries, power-to-gas, power-to-liquid) [4]. Key requirements for these technologies include rapid charge/discharge rates, high energy density, long life cycle, stable operation and performance and cost-effectiveness. The specific requirements for each type of energy storage depend on the type of application for which it is intended for. Few options are currently available for large-scale storage, mainly pumped storage hydropower (PSH) systems that utilise elevation changes to store off-peak electricity for later use [5]. However, the possibility of implementing this technology is limited to locations with favourable geography, meaning that alternative technologies are needed. Power-to-gas (PtG) systems, and more specifically power-to-methane (PtM) systems are gaining particular attention, especially in regions where a natural gas infrastructure is already available. Fig. 1 shows the general structure of a PtM plant and its three components: (1) the electrolysis unit, (2) the CO_2 separation unit and (3) the methanation unit.

* Corresponding author.
E-mail address: tmendiara@icb.csic.es (T. Mendiara).

https://doi.org/10.1016/j.enconman.2022.115866
Received 14 March 2022; Received in revised form 20 May 2022; Accepted 5 June 2022
Available online 16 June 2022

Characteristics of a PtM system:

- The PtM unit stores surplus renewable electricity in the form of hydrogen through electrolysis
- Hydrogen is not used to produce electricity again but to produce methane. Thus, hydrogen is fed together with CO_2 into a methane generation process via Sabatier reaction (methanation)
- A CO_2 source is required
- The methane produced can be: i) used to generate power when demand overbalances supply, ii) injected into the natural gas grid, iii) used in the transport sector

Therefore, unlike PSH, there is no strict requirement to balance electricity input and output in PtM systems since surplus electricity is stored in the form of hydrogen. Moreover, the fact that PtM units can flexibly store different amounts of energy depending on the surplus generated also favours sector coupling. In recent years, the number of existing PtM projects and plants in the EU has increased, and it continued growth is expected given the environmental goals set for 2050. Recent estimates show a total of 73 PtM plants across Europe, 37 which use chemical methanation (Sabatier reaction) with the remainder using biological methanation [6]. Recent reviews detailing the current state of the technologies available for electrolysis and methanation units can be found elsewhere in literature [7–9]. The most recent studies are focused on the scale-up and techno-economic analysis of PtM systems. For most of the PtM configurations considered, the main expenditures are related to the purchase of electrical energy and the capital expenditure and operating expenses derived from the electrolyser while the impact of the CO_2 source and the methanation unit is limited [10]. Thus, the economic viability of PtM systems can be improved by ongoing technical developments and by the use of co-products, such as oxygen from electrolysis and electricity [10,11].

An additional advantage of PtM technology, and one that is of great interest, is the possibility it offers for CO_2 utilization [12]. Biogas production, tail gas from power plants or industrial processes, direct air capture and geothermal units have been proposed as sources for the CO_2 to be supplied to the PtM system [4,13]. This paper evaluates the alternative of supplying PtM with the CO_2 streams generated by advanced carbon capture technologies. The incorporation of carbon capture into the methanation process has shown to be an economically viable technology for the production of fuels [14]. Carbon capture technologies are commonly applied to large-scale facilities, such as power stations, and allow to produce a concentrated stream of CO_2 that can later be stored or used [15]. We focus on one of these technologies, known as chemical looping combustion (CLC) technology, which is noteworthy for having low energy and economic costs associated with CO_2 capture [16], compared to other carbon capture approaches such as the widespread method of CO_2 capture by flue-gas scrubbing with amines. We propose the incorporation of CO_2 from the CLC of biomass (bioCLC) as the CO_2 source for PtM systems, which we refer to hereafter as PtM-bioCLC process. Biomass combustion has frequently been included in recent PtM schemes since it can be considered renewable carbon [17,18]. According to a comprehensive techno-economic analysis by Peters et al. [12] of different scenarios for the development of PtM systems including different CO_2 sources, the possibility of using CO_2 from carbon capture processes becomes considerable when the price of CO_2 from industrial sources is above €35/tonne CO_2. Since the cost per tonne of CO_2 emitted in Europe is experiencing a meteoric rise unlike any period since the introduction of the EU emissions trading system in 2005, reaching a maximum of €97/tonne CO_2 in February 2022 [19], PtM-bioCLC can be regarded as a promising technological option. The present work aims to assess the environmental viability of the PtM-bioCLC process for the first time. Life cycle assessment (LCA) was chosen as a tool for this purpose, as it allows the environmental benefits and hazards of PtM-bioCLC to be identified in comparison with those of conventional processes producing the same products. LCA addresses the environmental aspects of the complete chains of product systems (cradle-to-grave analysis) and is also comprehensive with respect to the number of environmental impacts, which include the environmental issues most often related to energy conversion systems [20].

2. Background

2.1. BioCLC in the in PtM-bioCLC system

As a result of the intense development and maturity of CLC technology over the last 20 years, it has now reached a technology readiness level of 6–7 [21]. In CLC, full oxidation of fuel to CO_2 and H_2O is achieved and the energy released is used for heat/electricity production. CLC has been already demonstrated for all types of fuels (gas, liquids and solids). CLC prevents mixing of fuel and air since the oxygen required for combustion is supplied by a solid oxygen carrier (M_xO_y) circulating between two reactors, commonly fluidized beds [22]. Inside one of the reactors (fuel reactor), the oxygen carrier reacts with the fuel as it is being reduced (M_xO_{y-1}) while the fuel is being oxidized to CO_2 and H_2O. In the other reactor (air reactor), the reduced oxygen carrier is reoxidised in air and becomes ready to start a new cycle and therefore maintain the continuous combustion of the fuel. The same energy is released in the CLC as by conventional combustion. There are two different configurations for burning biomass in a CLC system [23]: i) the chemical looping with oxygen uncoupling (CLOU) and ii) the *in situ* gasification chemical looping combustion (*i*G-CLC). The difference

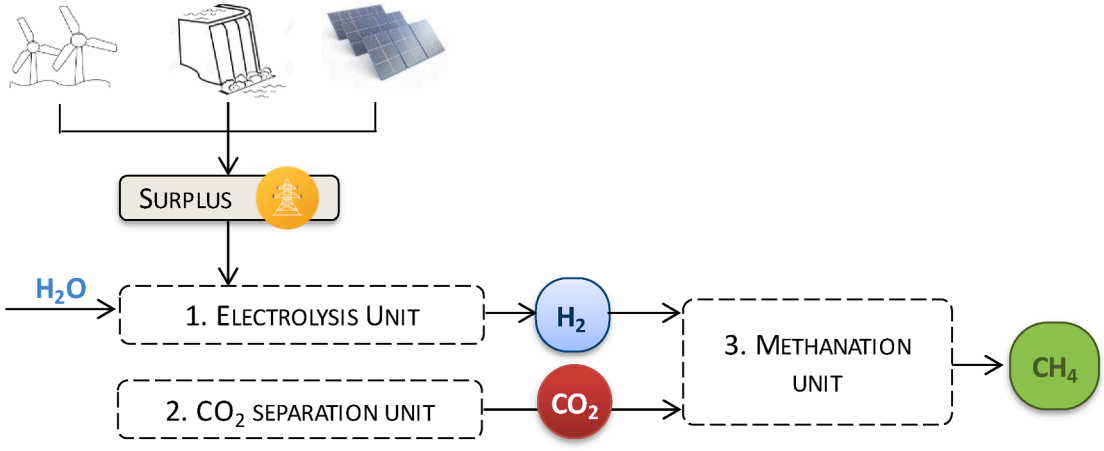

Fig. 1. Schematic diagram of the power-to-methane system (PtM).

between CLOU and *i*G-CLC is the type of process that takes place in the fuel reactor. In CLOU mode, the oxygen carrier is able to generate gaseous oxygen (O_2) under fuel reactor conditions after which, both volatiles and char react with O_2, similarly to conventional biomass combustion in air. In *i*G-CLC mode, either steam or CO_2 must be supplied to gasify the biomass char after volatile release. Both volatiles and char gasification products (H_2/CO) subsequently react in a gas–solid reaction with the oxygen carrier to produce CO_2 and H_2O. The type of oxygen carrier used in the different combustion modes is tipically different. While low-cost materials -mainly Fe-based or Mn-based minerals or industrial residues- are used in *i*G-CLC, synthetic materials based on copper and/or manganese oxides are preferred for CLOU [24]. These synthetic materials are produced by different methods, mainly impregnation on a support, granulation or spray-drying [22]. The different nature of the oxygen carriers will have implications for the LCA of the processes, together with the lifetime of the respective materials. Lifetime is linked to losses of in the oxygen carrier due to particle attrition or deactivation in the CLC system and determines the make-up flow that should be supplied. This make-up flow is seen as one of the main contributions to the cost of CO_2 capture in CLC [25]. Nevertheless, the cost of CO_2 capture in CLC is estimated to be among the lowest of all carbon capture processes. Moreover, the environmental impact resulting from the disposal of the elutriated material should be also considered [26,27]. In the case of synthetic materials, recovery of the active phase from the spent material has been evaluated as an option to minimise this impact [27].

Fig. 2 is a schematic diagram of the PtM-bioCLC process analysed in the present work. This approach has some additional advantages compared to other PtM configurations:

- PtM-bioCLC allows advantage to be taken of renewable discharges together with CO_2 utilisation while producing a renewable fuel in addition to electricity.
- PtM-bioCLC facilitates our ability to achieve net zero emissions or even negative CO_2 emissions, defined as the removal of previously emitted CO_2 from the atmosphere. This could be accomplished if part of the CO_2 generated in biomass combustion is stored, since this CO_2 was already taken from atmosphere during plant photosynthesis.

Only one study was found in the literature that conducted LCA of a PtM scheme in which CLC was proposed as the carbon capture technology to produce energy and as a source of CO_2. In this study by Bareschino et al. [28], hydrogen was also produced by renewable electricity. A copper-based oxide supported on zirconia was used as the oxygen carrier and it was able to work in CLOU mode. The important difference with respect to the present study is that these authors considered coal as the fuel for the CLC process, thus increasing the impact on climate change. In addition, the PtM-bioCLC process in the present work was designed in such a way that the electricity produced by the CLC system replaces the power that could be generated by the combustion of the hydrogen produced by electrolysis in a gas turbine. This aspect of process integration is not considered in the work by Bareschino et al. [28].

2.2. LCA of PtM systems

Several studies can be found in the literature regarding LCAs previously conducted on different configurations of PtM systems. They considered different system boundaries, functional units, origins of the electricity used in the electrolysis step and CO_2 sources. However, interesting general conclusions can be reached from the studies to date:

- The amount and type of electricity supplied to electrolysis represents the largest contribution towards the LCA results of a PtM system, more so than the different CO_2 sources [29].
- Many of the studies conclude that the use of renewable electricity for production of H_2 is essential for positive environmental performance [30]. A number of them even point to wind or hydropower discharges as the most beneficial [29,31,32].
- The load hours of PtM systems significantly influences LCA results [33].
- Different CO_2 sources can be considered: flue gas from power stations, the cement industry, biogas upgrading, CO_2 extracted from ambient air and geothermal units [13,31,34,35].
- The highest greenhouse gas emission benefit is attained when biogenic and atmospheric sources are provided [34].

Besides these general findings, specific LCA studies including CO_2 from carbon capture in flue gas from power plants present these main conclusions:

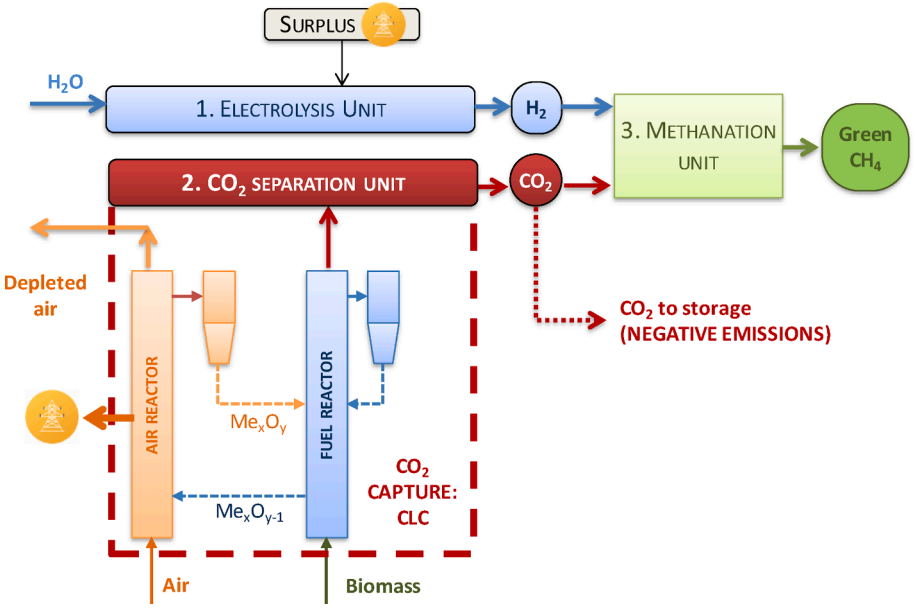

Fig. 2. Schematic diagram of the PtM system incorporating bioCLC as the CO_2 source (PtM-bioCLC).

- Flue gas from coal combustion was generally considered, except in the study by Zhang et al. [31]. According to the findings of these authors, the CO_2 captured from a wood-fired power station can achieve the highest reduction in greenhouse gas (GHG) emissions, even more than when CO_2 is captured from air.
- Amine scrubbing with monoethanolamine (MEA) was mostly assumed to be the carbon capture technology utilised for CO_2 capture.

From points presented above, the source of CO_2 can be expected to be significant when considering the integration of the PtM process into the energy production/consumption system. For example, some processes are able to produce energy –power plant with CO_2 capture– while other processes demand energy –direct air capture.

Considering all these results from previous LCAs, our study aims to contribute to a further exploration of the possibilities of CLC technology in PtM systems under the most favourable conditions. As it has been previously mentioned in the description of the PtM-bioCLC process, CLC with biomass as fuel is proposed as the CO_2 source and only surplus renewable electricity is used as the electricity source for the electrolysis step. Furthermore, the present study will consider the effects of operating under both CLOU and *i*G-CLC modes.

3. Methods

This LCA is based on the material and energy flows required by the PtM-bioCLC system. This section details, the scope definition, inventory analysis and impact assessment considered for the previously defined PtM-bioCLC systems.

3.1. Scope definition

The LCA presented in this paper follows the recommendations given by the European Platform on Life Cycle Assessment [36]. The scope of the study includes all the process steps outlined in Fig. 2. The steps considered are electrolyser and methanation reactor operation, oxygen carrier manufacturing and recovery/disposal after use, and CO_2 capture and eventual storage. GaBi® 9.5 Pro. software was used for the LCA simulation, together with the databases associated with this program.

3.1.1. Functional unit and base case

In this work, a comparative LCA was conducted with reference to the base case in Fig. 3(A). Accordingly, both the base case and the PtM-bioCLC alternatives were assumed to deliver the same products [33,37] and all calculations were based on having the same functional unit, consisting of an electrolyser using surplus energy from 500 MW_e of renewable sources for one year ($4.4{\cdot}10^6$ MWh), considering the expected renewable mix in Spain by 2030: 30% wind energy, 23% hydropower and 47% photovoltaic energy [38]. In the base case, Fig. 3(A), surplus generated energy was stored and then used for electricity production in a gas turbine ($1.69{\cdot}10^6$ MWh) when required. In the CLC cases, namely CLOU and *i*G-CLC using synthetic or mineral oxygen carriers in Fig. 3(B) to (D), the electrical energy generated by burning biomass was the same as that produced in the hydrogen turbine for the base case.

However, hydrogen was not used for electricity generation in the CLC cases, instead, it was used to produce CH_4 by combining with part of the CO_2 captured in the CLC unit. Therefore, the CH_4 produced was defined by the H_2 generated in the electrolyser. The same amount of CH_4 was considered to have been used in all cases ($1.82{\cdot}10^8$ kg); however, whereas the CH_4 was of fossil origin in the base case, it was produced from renewable sources in the proposed cases. Excess CO_2 was produced by CLC after deducting the amount required by the methanation process. This surplus CO_2 surplus was stored, counting as negative CO_2 emissions.

3.1.2. System boundaries

System boundaries defined the limits for the input and output flows of material and energy considered in the LCA. These boundaries were defined following these considerations:

- According to the recommendations given in the literature, no emissions were counted for the combustion of biomass since the carbon in biomass was fixed by photosynthesis. Nevertheless, indirect greenhouse gas (GHG) emissions originating in biomass growth were considered [34]. The fraction of carbon dioxide generated in biomass combustion and not used in the Sabatier process was assumed to be stored, thus producing negative CO_2 emissions
- Impacts from extraction of raw materials and oxygen carrier make-up flows together with waste generation, energy recovery and oxygen carrier disposal were included
- Impacts of from H_2 or CO_2 transport from sources to the PtM system were not considered

3.1.3. Time and geographical references

The literature reports a decrease in the environmental impact of PtM systems when higher load hours were considered [33]. Thus, 8000 h/year operation was assumed for the CLC and methanation units (the electrolysis unit operated whenever there was surplus electrical energy). For better accuracy in the LCA, processes located in Spain were taken into consideration. Otherwise, data from the European Union or Germany were included.

3.1.4. Impact categories

GaBi 9.5® Pro. enabled calculation of 16 environmental impact indicators (EIIs) following the recommendations made by the European Comission-Joint Research Center [36]. The values obtained for each of these, along with the corresponding units and the method used for their estimation are presented in Table S1 in Supporting Information (SI). Selected impacts are grouped into level "I" (recommended and satisfactory), level "II" (recommended but in need of some improvements) or level "III" (recommended, but to be applied with caution).

3.2. Life cycle inventory (LCI)

3.2.1. H_2 production and water electrolyser

Hydrogen was produced in a proton exchange membrane (PEM) electrolysis unit whose main parameters are shown in Table 1.

Both water and electricity were required for the production of H_2 by electrolysis. The LCA considered reverse osmosis deionized water. The process data were also taken from the GaBi database.

3.2.2. CO_2 produced in bioCLC

In the PtM-bioCLC processes proposed in Fig. 3(B) to (D), a power generation unit based on CLC technology burnt biomass to produce electricity and CO_2, which was supplied together with the hydrogen obtained by electrolysis in order to allow the Sabatier reaction to proceed. The amount of CO_2 released during biomass combustion was calculated considering pine pruning biomass as fuel with an averaged chemical composition of 51.9 % carbon, 41.3 % oxygen, 6.3% hydrogen, and 0.5 % nitrogen and combustion enthalpy of 18.14 MJ/kg [41]. Different materials were considered as oxygen carriers depending on the particular CLC operation mode. For CLOU, a synthetic material based on CuO (Cu60) was considered [42]. For *i*G-CLC mode, both a CuO-based (Cu15) synthetic material [43] and the mineral ilmenite ($FeTiO_3$) were included, leading to two different processes, referred to as *i*G-CLC_sOC and *i*G-CLC_mOC, respectively. All these materials have shown good performance for biomass combustion in different experimental campaigns in continuous CLC units up to the kW scale, in the case of CLOU, and MW scale in the case of *i*G-CLC [24]. Table 2 summarizes the properties and the preparation methods followed for oxygen carrier manufacturing.

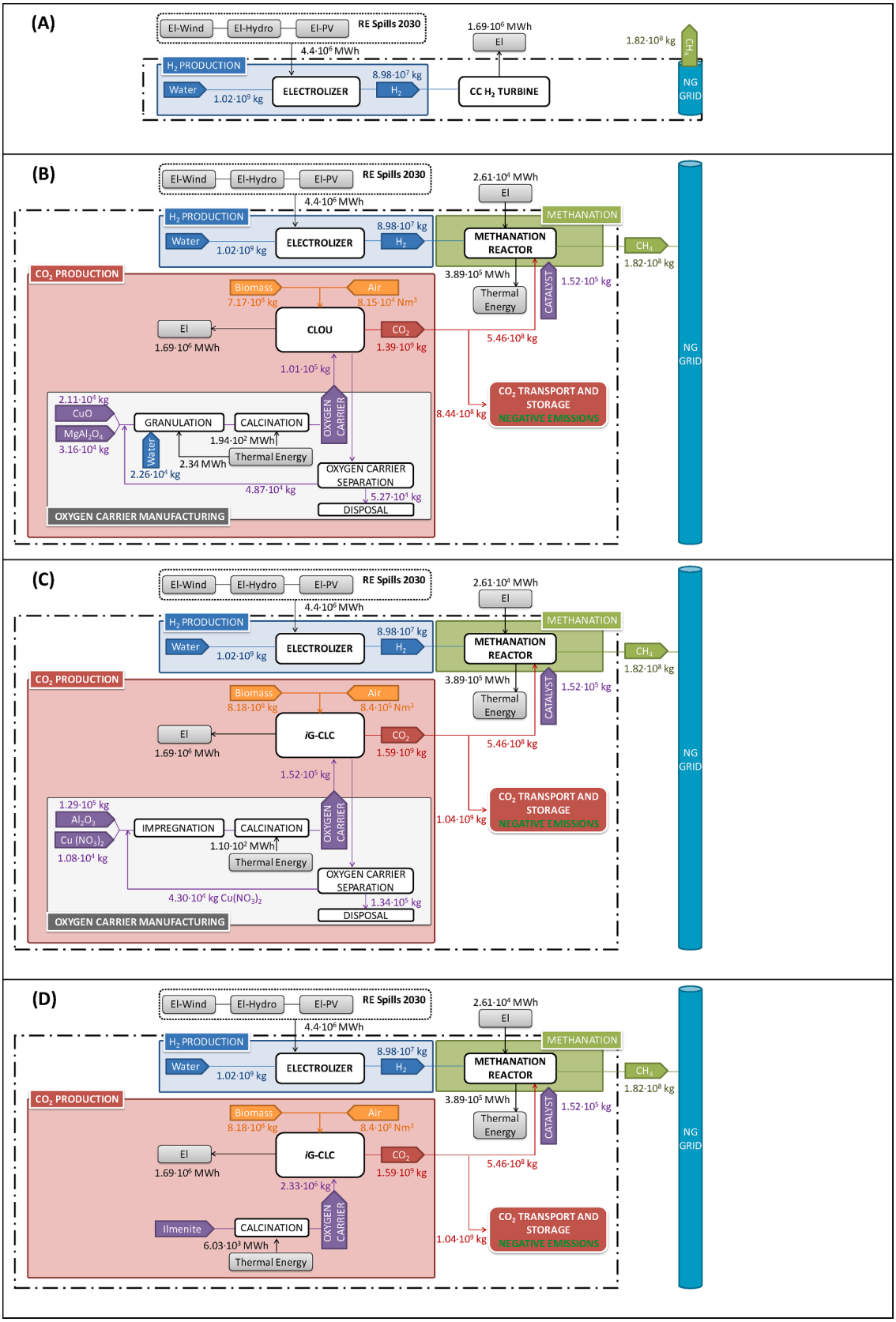

Fig. 3. Life cycle boundaries (black dash-dot line) of (A) Base Case and PtM-bioCLC process for (B) CLOU mode (C) *i*G-CLC mode with synthetic oxygen carrier (*i*G-CLC_sOC) (D) *i*G-CLC mode with mineral oxygen carrier (*i*G-CLC_mOC).

Table 1
Main parameters used in H_2 production cases for PEM electrolysis [9,33,39].

Life time	[years]	10
Total electricity usage	[kWh/kg]	50.3
Cell temperature	[°C]	20–100
Cell voltage	[V]	1.8–2.2
Net system electrical efficiency		66 %
Plant capacity	(kg/day)	1500
Hydrogen outlet pressure	[kg/m^2]	4882
Electrolyte		Solid polymer membrane (Nafion)
Charge carrier		H_3O^+/H^+

Cu60 consisted of 60 wt% CuO supported on $MgAl_2O_4$ spinel and was prepared using the spray drying/granulation technique [42]. The spray-drying/granulation mechanism is based on moisture elimination, for which the feed product was subjected to a heated atmosphere. A solution was pumped to an atomizer, in order to break up the liquid feed into a spray of fine droplets that were propelled into a drying gas chamber where the moisture vaporisation then occurred, resulting in the formation of dry particles. Finally, using an appropriate device, the dried particles were separated from the drying medium and collected in a tank. Once produced, the Cu60 particles were calcined for 24 h at 1100 °C. Cu15 was prepared by the incipient wetness impregnation method. This involved the addition of a volume of saturated copper nitrate corresponding to the total pore volume of the γ-Al_2O_3 acting as support. After impregnation, the particles were calcined at 550 °C in air to decompose the impregnated $Cu(NO_3)_2$ to CuO. After nitrate decomposition, the particles were calcined at 950 °C for 1 h [43]. Ilmenite is a mineral mainly composed of $FeTiO_3$. After extraction, crushing and sieving, it was calcined for 24 h at 1100 °C to complete its oxidation to pseudobrookite (Fe_2TiO_5). It was assumed that 80 % of the Cu60 oxygen carrier used for CLOU was recovered and sent back to granulation. Also, 80 % of the Cu15 oxygen carrier was assumed to have been recovered with nitric acid. In both cases, 20 % of the oxygen carrier was sent to landfill. Used ilmenite was sent to landfill with no recovery. Table 3 shows the electrical efficiencies for the CLOU/*i*G-CLC processes with biomass.

3.2.3. CH_4 synthesis via Sabatier reaction

Hydrogen produced by water electrolysis can react with CO_2 to produce methane according to the Sabatier reaction:

$$4\,H_2 + CO_2 \rightarrow CH_4 + 2H_2O \quad \text{(R1)}$$

The main parameters of Sabatier reaction are shown in Table 4.

4. Results

4.1. Global Warming potential and Resource Use-Depletion

First, the LCA indicators Global Warming Potential (GWP) and those under the general category Resource Use-Depletion are shown in Figs. 4 and 5, respectively, since they are considered key drivers for the development of the PtM process, compared to other energy storage options. Numerical values for the indicators are given in Table S2 of Supporting Information (SI). In Fig. 4, the final GWP values for the base case and the PtM-bioCLC systems are shown, together with a breakdown of this value by the different processes included in Fig. 3 for each system: hydrogen production, natural gas extraction, biomass production/extraction, methanation through the Sabatier reaction, CO_2/electricity production by CLC and eventual CO_2 storage leading to CO_2 negative emissions. Fig. 4 shows that there is a significant difference between the GWP values corresponding to PtM-bioCLC configurations (i.e. CLOU and *i*G-CLC_sOC/*i*G-CLC_mOC) when compared to the base case. While the GWP value in the base case is positive, negative values are achieved in all the PtM-bioCLC cases. The difference in absolute value is also significant (more than 400%): values drop from $2.62{\cdot}10^8$ for the base case to $-8.62{\cdot}10^8$, $-1.06{\cdot}10^9$ and $-1.05{\cdot}10^9$ kg CO_2 equivalent for CLOU, *i*G-CLC_sOC and *i*G-CLC_mOC, respectively.

The figure also indicates that this change to negative final GWP values is mainly attributed to the negative emissions produced by all the CLC processes owing to the storage of the CO_2 not consumed in the methanation unit (see Fig. 3) and, to a much lower extent, to the avoidance of methane extraction. Other processes, such as hydrogen production and biomass production/extraction have the largest positive contribution to the GWP associated with the PtM-bioCLC configurations.

Another fact underlined by Fig. 4 is that the differences between the GWP values of the CLC processes (i.e. CLOU and *i*G-CLC) can be attributed to the different biomass supply requirements for combustion. In order to generate the same amount of electricity, larger volumes of biomass are required by the process with lower combustion efficiency, i.e. the iG-CLC process. The combustion of larger amounts of biomass leads to more CO_2 being produced. Since the amount of CO_2 required by the methanation process is the same regardless of the CLC process where it originates, this results in larger amounts of CO_2 sent to storage (negative emissions) in the case of *i*G-CLC. As previously explained, since CO_2 storage is the process with the greatest influence over the final GWP value, more overall negative GWP values were obtained for the *i*G-CLC process than for CLOU.

Fig. 5 shows the values for the Resource Use-Depletion indicators land use (LU), water use (WU), resource use energy carriers (RUE) and resource use minerals and metals (RUM), together with their corresponding units for the two CLC modes with respect to the base case.

The value for LU is higher in the proposed PtM-BioCLC schemes due to the biomass extraction/production required in these cases, compared

Table 3
Electrical efficiencies for the PtM base case and alternative CLOU/*i*G-CLC processes with biomass.

	CO_2 capture (%)	Efficiency (%)	Ref.
CCGT (H_2 turbine)	–	56.8	[49]
CLOU with Cu60	100	46.8	[50]
iG-CLC with Cu15/Ilmenite	100	41 (ultra-supercritical)	[25,51,52]

Table 4
Main parameters used in CH_4 production (1 kg) by Sabatier reaction [33,40].

Operating temperature	[°C]	250
Operating pressure	[bar]	6–7
CO_2 input	[kg]	2.94
H_2 input	[kg]	0.51
Electricity input	[kWh]	0.33
H_2 output	[kg]	$9.00{\cdot}10^{-3}$
Heat output	[kWh]	3.01
CO_2 emissions	[kg]	0.19

Table 2
Main characteristics of the oxygen carriers used in the PtM-bioCLC processes.

Process	Oxygen carrier	Preparationmethod	MeO (%)	Lifetime (h)		T_{FR}-T_{AR} (°C)		Solids inventory (FR + AR) (kg/MW)		Recovery (%)
CLOU	Cu60	Spray drying	60	2500	[43]	920–900	[42]	200 + 100	[42]	80
iG-CLC_sOC	Cu15	Impregnation	15	2500	[43]	800–900	[44]	150 + 350	[45]	80
iG-CLC_mOC	Ilmenite	–	100	700–800	[46]	950–1050	[47]	850 + 250	[48]	0

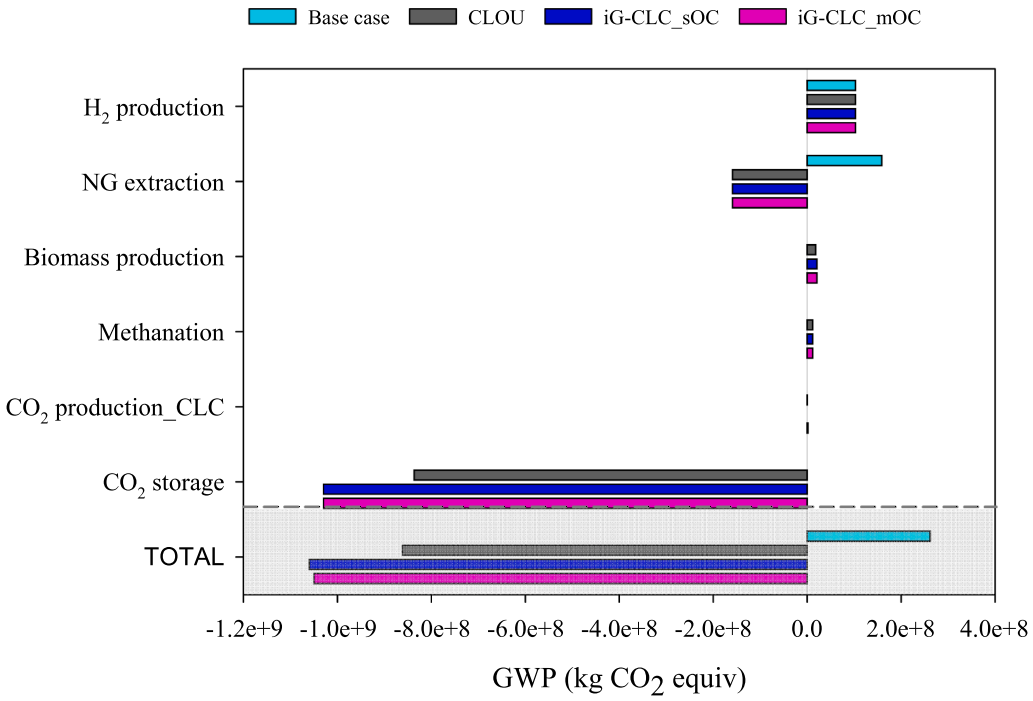

Fig. 4. GWP of the PtM-bioCLC process compared to the base case for CLOU, *i*G-CLC_sOC and *i*G-CLC_mOC operation modes.

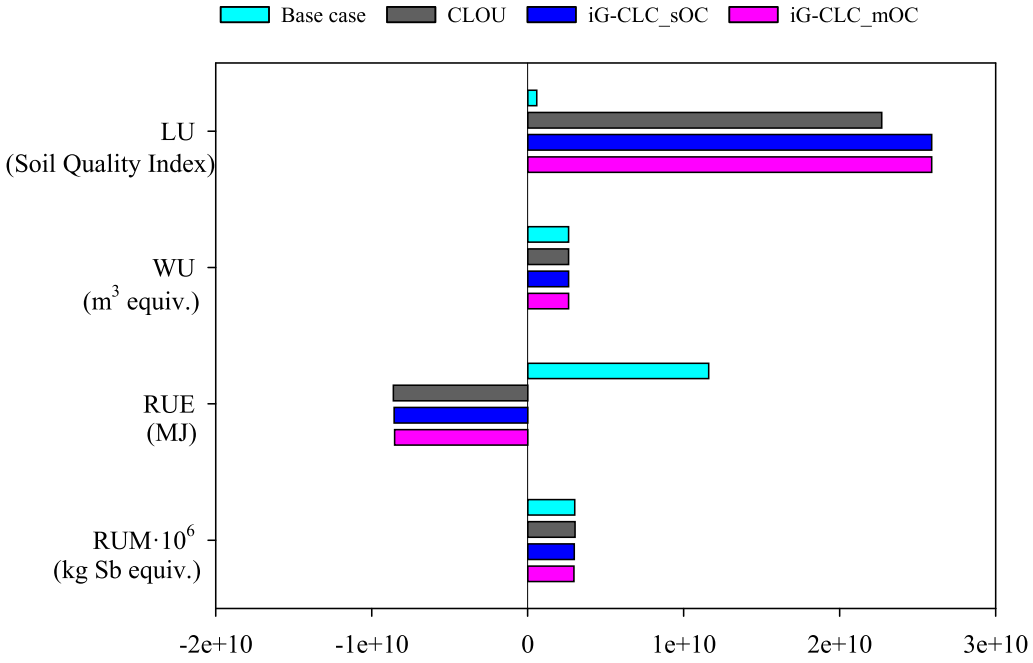

Fig. 5. Resource Use-Depletion indicators for the two modes for biomass combustion considered (iG-CLC and CLOU). Each indicator is expressed in its corresponding units indicated in Table S1 in Supporting Information.

to the base case. WU and RUM show little difference in relation to the base case. In the case of the RUM indicator, these results show that oxygen carrier extraction/manufacturing has little influence on this indicator. Nevertheless, RUE shows a significant decrease for the PtM-bioCLC processes compared to the base case since natural gas extraction is avoided.

Table 5 compares the results regarding GWP indicator in the present work with previous values reported in the literature for different PtM configurations. The table indicates the origin of the electricity used for electrolysis (renewable or mix including fossil-fuel derived energy) and the origin of the CO_2 used in methanation (fossil fuel or biogenic/atmospheric CO_2). All values are compared on the basis of 1 MWh CH_4 produced. For the same CO_2 origin, it is clear that the origin of the electricity used in electrolysis significantly affects the GWP values obtained. The highest GWP values were achieved when an energy mix that included fossil fuel-derived energy, was used (cases 5, 13 and 16 in Table 5). When the different origins of the CO_2 are taken into account, it can be seen that processes using CO_2 captured from the flue gases of power plants/industries seem to have larger GWP values (cases 1 to 8) than in the case where CO_2 is of biogenic origin obtained as the waste or

Table 5
Comparison of the GWP values obtained for PtM-bioCLC with values in the literature for other PtM configurations.

No.	Authors	H_2 production			CO_2 origin					GWP per MWh CH_4 produced	Ref.
		Renew.		Mix[a]	Coal power plant[b]	Cement[b]	Residue[b]	DAC	Biomass		
		Wind	PV							kg CO_2 equiv.	
1	Meylan et al.	X			X					157	[34]
2	Meylan et al.		X		X					205	[34]
3	Reiter and Lindorfer	X			X					105	[32]
4	Reiter and Lindorfer		X		X					191	[32]
5	Reiter and Lindorfer			X	X					**1076**	[32]
6	Sternberg and Bardow	X	X		X					799	[33]
7	Bareschino et al.	X			X					60	[28]
8	Chauvy et al.	X	X			X				130	[53]
9	Meylan et al.	X					X			53	[34]
10	Meylan et al.		X				X			99	[34]
11	Reiter and Lindorfer	X					X			22	[32]
12	Reiter and Lindorfer		X				X			108	[32]
13	Reiter and Lindorfer			X			X			**994**	[32]
14	Meylan et al.	X						X		54	[34]
15	Meylan et al.		X					X		134	[34]
16	Parra et al.			X				X		**406**	[29]
17	Navajas et al. (CLOU)	X	X						X	**−341/-10**[c]	This work
18	Navajas et al. (iG-CLC_sOC)	X	X						X	**−418/−9**[c]	This work
19	Navajas et al. (iG-CLC_mOC)	X	X						X	**−471/−8.5**[c]	This work

[a] Including fossil-fuel derived energy.
[b] CO_2 capture by amine scrubbing.
[c] Values with and without CO_2 storage.

by-product of a process, e.g. biogas upgrading (cases 9 to 13), even when the CO_2 capture in all the cases was by amine absorption, which is a highly energy-demanding process. Moreover, when CO_2 is of biogenic origin (produced as a waste or by-product of a biogenic process, captured from air or generated by biomass combustion) it is possible to achieve negative GWP values. Nevertheless, this is only the case for the results in the present study involving the combustion of biomass (cases 17 to 19). Even when there was no storage of the excess CO_2 produced by bioCLC, the results in Table 5 for the CLOU, *i*G-CLC_sOC and *i*G-CLC_mOC processes present negative GWP values per MWh methane produced (−10, −9 and −8.5 kg CO_2 equiv./MWh CH_4 produced, respectively). These GWP values are the lowest reported to date using renewable energy surplus to produce hydrogen by electrolysis. This demonstrates the potential of the proposed PtM-bioCLC configuration for the reduction of GHG emissions compared to many the other PtM configurations proposed to date.

With regard to the Resource Use-Depletion indicators, the proposed PtM-bioCLC configurations presented lower values (even negative in the case of RUE, as shown in Fig. 5) than those reported in the study by Bareschino et al. [28] (case 7 in Table 5), which also considered CLC technology as a CO_2 source. However, no details were given by Bareschino et al. regarding oxygen carrier recovery and/or disposal, which could also affect these differences.

By way of conclusion, it can be said that the PtM-bioCLC configurations proposed in this work significantly decrease the GWP and Resource-Depletion values that have been associated with the PtM process until now. The incorporation of bioCLC (both CLOU and *i*G-CLC) as a CO_2 source could therefore offset the loss of efficiency attributed to methanation, as well as reduce the energy demand for CO_2 separation/capture that has traditionally penalised other PtM configurations

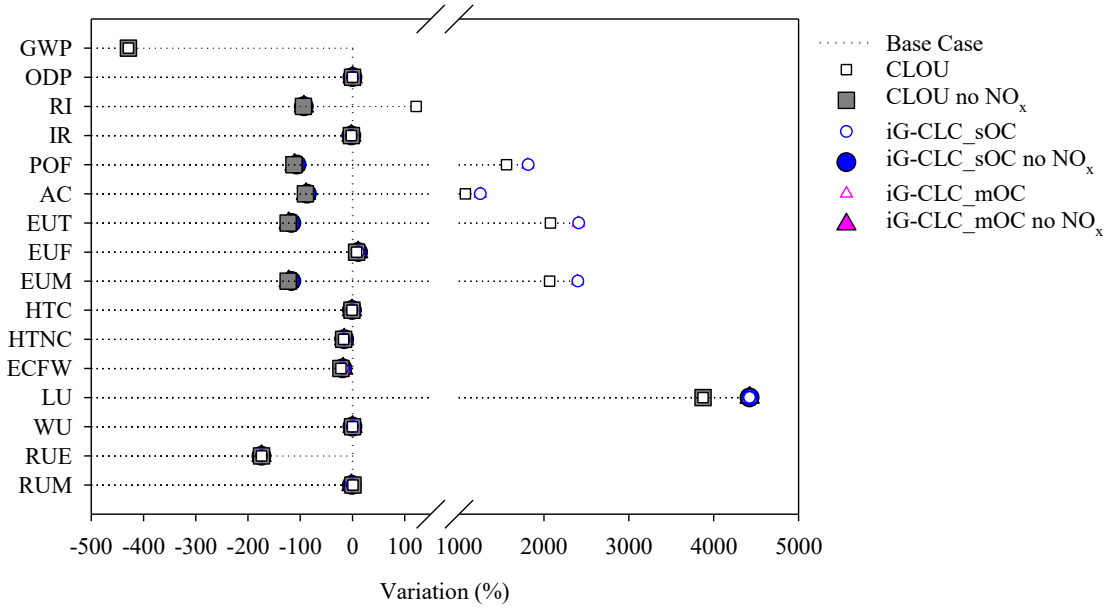

Fig. 6. Percentage of variation of other LCA indicators with respect to the base case in Fig. 3.

described to date.

4.2. Other environmental impacts

Fig. 6 shows the variation in the remaining LCA indicators considered with respect to the base case for the two CLC modes used in the PtM-bioCLC configurations. The values of the corresponding indicators are included in Table S2 in Supporting Information (SI). This variation is expressed as percentage change with regard to the value reached for the same indicator in the base case, which is why the base case is represented as a vertical dotted line at x = 0 in the figure. Apart from the previously analysed GWP and Resource Use-Depletion indicators, the figure includes other indicators from other impact categories: photochemical ozone formation (POF) and ozone depletion potential (ODP); the human health categories of respiratory inorganics (RI) and ionising radiation (IR); acidification potential (AC); the eutrophication categories of terrestrial eutrophication (EUT), freshwater eutrophication (EUF) and marine eutrophication (EUM); the human toxicity categories of carcinogenic toxocity (HTC) and non-carcinogenic human toxicity (HTNC); and freshwater ecotoxicity (ECFW).

In order to perform an accurate analysis of the effect of the PtM-bioCLC schemes on the different LCA indicators, previous studies by the authors were taken into consideration. The main contributor to NO_x formation in CLC is fuel-N [22]. Fuel-N is released during biomass devolatilisation in the fuel reactor as NH_3 and HCN, which can evolve into N_2 or NO depending on the combustion conditions. Char-bound nitrogen can evolve into NO, N_2O or N_2, although N_2O decomposes to N_2 at temperatures higher than 900 °C. It was shown that in CLC, operating under both CLOU and *i*G-CLC and with different types of biomass, fuel-N was mostly found in the fuel reactor as N_2 owing to combustion conditions there [54]. Thus, no NO_x emissions were considered for the PtM-bioCLC systems in the present work. This is reflected in Fig. 6, where open symbols represent the values of the indicators if NO_x was emitted as in the conventional combustion of biomass, while closed symbols represent the non-formation of NO_x, corresponding to the cases of bioCLC. As seen in Fig. 6, half of the LCA indicators remain similar to the corresponding value in the base case regardless of whether NO_x emissions are considered or not. The consideration of NO_x emission does not affect the values of GWP and RUE indicators either, which are significantly lower than the base case, as previously explained before. However, when NO_x emissions are not considered, the RI, POF, AC and EUT and EUM indicators experience a significant change from values much higher than those in the base case (variation ~ 2000%) to values much lower than this reference (variation ~ −100%). The only indicator not affected by NO_x emissions and with a value much higher than the base case is LU. The higher values obtained for the studied PtM-bioCLC systems can be attributed to biomass extraction/production requirements for the CLC process.

Previous LCA studies of PtM systems concluded that while these processes could reduce their climate change impact (GWP), they can also be detrimental in other categories, such as eutrophication or toxicity-related impacts [30]. Nevertheless, as shown by the results in Fig. 6 and previous discussion, this is not the case of the PtM-bioCLC configurations proposed in the present work, given that the values of 15 out of the 16 LCA indicators calculated for the CLOU, iG-CLC_sOC and iG-CLC_mOC are similar to or much lower than those obtained for the indicators in the base case.

4.3. Hotspots analysis

This section identifies the processes and/or flows responsible for a significant share of an overall impact for all LCA indicators and their respective impacts that were previously compared. As was the case in Fig. 4, the processes considered were the production of H_2 by electrolysis, biomass production, the methanation process based on Sabatier reaction, natural gas extraction and CO_2 production for methanation by bioCLC as well as the storage of the excess of CO_2 produced. These results are shown in Fig. 7 for the CLOU, iG-CLC_sOC and iG-CLC_mOC operating modes. Some differences can be appreciated between them. In the case of operation under CLOU mode, the RUM indicator shows a small contribution to the final value from the CO_2 produced by CLC that is not observed in the *iG*-CLC processes. This can be associated with the intensive use of CuO in the manufacturing of the Cu60 oxygen carrier, more so than in the preparation of Cu15, despite the assumption for both CuO-based oxygen carriers that most of the copper in them was recycled after use to produce new oxygen carrier via a new granulation or impregnation process. In the case of operation under *i*G-CLC_sOC, the RI, POF, AC, EUT and EUM indicators present a contribution to the final

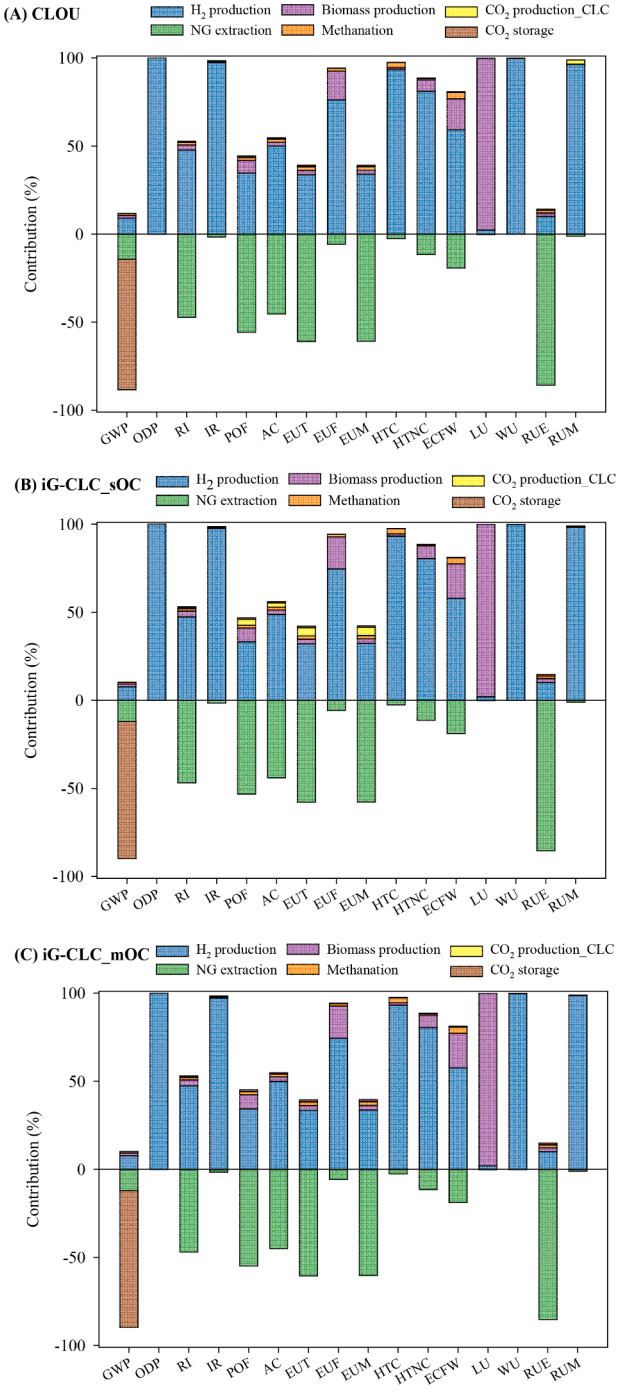

Fig. 7. Contribution of each process to the overall value of the indicator (A) CLOU (B) *i*G-CLC_sOC and (C) *i*G-CLC_mOC.

value from the CO_2 produced by CLC that is not observed in remaining processes. This is due to the release of NO_x during oxygen carrier manufacturing through the impregnation process. As previously explained, calcination of the impregnated oxygen carrier is required to decompose $Cu(NO_3)_2$ into CuO, with the corresponding NO_x released into atmosphere.

However, similar trends can be also found when comparing the results in Fig. 7(A) to (C). Generally, the processes that have more influence on the LCA indicators are said to be H_2 production, natural gas extraction and biomass production together with the storage of the excess CO_2. The methanation process and CO_2 production by bioCLC have little influence on the final results.

The main contributors to the final value of the indicators ODP, IR, HTC, ECFW, WU and RUM were the generation of hydrogen by electrolysis of water and, more specifically, the use of different renewable energies: photovoltaic (ODP, IR, ECFW, RDM), wind and hydropower (HTC), and hydropower (WU). The latter result highlights the influence that the type of electricity considered had on the LCA and is in line with previous results found in the literature where the amount and type of electricity supplied to electrolysis accounted for more than 90% of the LCA results for all indicators [29]. The avoidance of natural gas extraction in the PtM-bioCLC configurations exerts the most influence on the RUE parameter, making it strongly negative, as previously seen in Fig. 5.

The high impact of electrolysis production or the avoidance of natural gas extraction on the LCA is a factor common to any other PtM system considered in the literature [32]. However, as regards the PtM-bioCLC configurations proposed in this work, greatest impact in the LCA of the process can be specifically attributed to both the use of biomass as the source of the CO_2 used in methanation and the storage of the excess CO_2 produced. The latter only affected the GWP value by making it strongly negative. On the other hand, for all the PtM-bioCLC schemes analysed in Fig. 7, it is clear that biomass extraction/production affected a significant number of parameters, such as RI, POF, EUF, HTNC, ECFW and finally LU. Actually, the value of LU was almost exclusively determined by the impact of biomass extraction and was the only parameter that incremented its value when PtM-bioCLC cases were compared with base case (Fig. 6). In order to investigate how the origin of biomass influenced the value of the LU parameter, an additional analysis was performed. The values of this indicator under the LCA conditions in the present work, which would correspond to the biomass extraction process in the PtM-bioCLC chain, were calculated for two additional types of biomass: wheat straw and olive tree pruning material. Fig. 8 shows the relative value obtained for the extraction/production per MWh biomass including the pine pruning material used in the analyses of the indicators for comparison. According to the figure, large differences may be expected in the LU indicator depending on the type of biomass considered for CLC. Apparently, forest residues (pine pruning) may have much lower impact on land use than any of the agricultural residues considered.

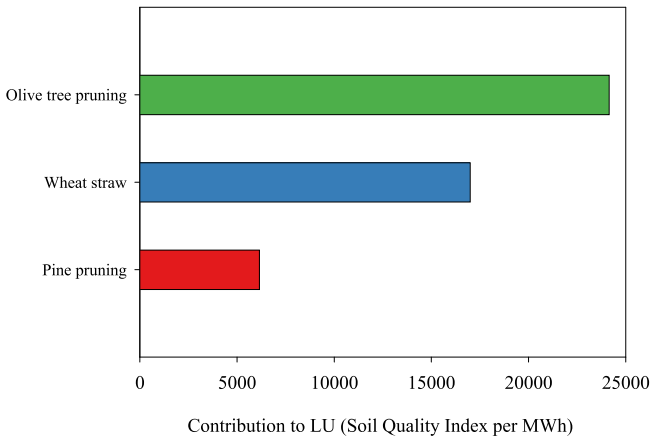

Fig. 8. LU associated to the extraction/production of 1 kg biomass per MWh produced: pine pruning material (based on [55]) and wheat straw and olive tree pruning material (based on [56]).

5. Conclusions

LCA was conducted on the environmental impact of configurations for PtM-bioCLC systems that obtain CO_2 for methanation via a CLC system burning biomass in the present work. Two different CLC modes were considered, namely CLOU and *i*G-CLC. Two different types of oxygen carrier were considered for *i*G-CLC: mineral (*i*G-CLC_mOC) and synthetic (*i*G-CLC_sOC).

Up to sixteen indicators were considered in the LCA. With regard to climate change impact, evaluated through GWP indicator, the proposed configurations achieved the lowest value for this indicator among the different configurations studied in the literature. Moreover, a negative GWP value is reached in all cases, which means that this new process would facilitate the removal of previously emitted CO_2, thus achieving negative emissions and making PtM-bioCLC a promising PtM scheme to be considered in the future development of these technologies.

With regard to Resource Use-Depletion indicators, WU and RUM were barely changed with respect to the base case. However, RUE indicator was significantly lower, given that natural gas extraction is avoided through the PtM-bioCLC processes when compared to the base case.

More specifically, the values for RI, POF, AC and EUT and EUM indicators were significantly lower. These indicators are influenced by the amount of NO_x emitted during biomass combustion. In the case of bioCLC, the nitrogen entering the CLC system is released in the form of N_2, preventing NO_x emissions and reducing their impact on the above-mentioned indicators. This represents an additional advantage for the proposed PtM-bioCLC configurations.

Further analysis of the contribution of each PtM stage to the final value of each LCA indicator, determined that the generation of CO_2 via bioCLC had a very limited influence on those values. The processes that most influenced the LCA indicators were H_2 production, together with biomass production, natural gas extraction and CO_2 storage. Avoidance of natural gas extraction made the RUE parameter negative. The LU value was almost exclusively determined by the impact of biomass extraction.

CRediT authorship contribution statement

Alberto Navajas: Conceptualization, Methodology, Validation, Formal analysis, Investigation, Data curation, Writing – review & editing. **Teresa Mendiara:** Conceptualization, Methodology, Validation, Formal analysis, Investigation, Data curation, Writing – original draft, Writing – review & editing, Supervision. **Luis M. Gandía:** Conceptualization, Methodology, Validation, Formal analysis, Investigation, Resources, Writing – review & editing, Visualization, Supervision, Project administration, Funding acquisition. **Alberto Abad:** Conceptualization, Methodology, Validation, Formal analysis, Investigation, Resources, Writing – review & editing, Visualization, Supervision, Project administration, Funding acquisition. **Francisco García-Labiano:** Conceptualization, Methodology, Validation, Formal analysis, Investigation, Resources, Writing – review & editing, Visualization, Supervision. **Luis F. de Diego:** Conceptualization, Methodology, Validation, Formal analysis, Investigation, Resources, Writing – review & editing, Visualization, Supervision.

Declaration of Competing Interest

The authors declare that they have no known competing financial interests or personal relationships that could have appeared to influence

the work reported in this paper.

Acknowledgments

This work was supported by Grant PDC2021-121190-I00 funded by MCIN/AEI/10.13039/501100011033 and by the European Union NextGenerationEU/PRTR and also by Grant PID2020-113131RB-I00 funded by MICIN/AEI/10.13039/501100011033. A.N. and L.M.G. gratefully acknowledge Grant RTI2018-096294-B-C31 funded by MCIN/AEI/10.13039/501100011033 and "ERDF A way of making Europe".

Appendix A. Supplementary data

Supplementary data to this article can be found online at https://doi.org/10.1016/j.enconman.2022.115866.

References

[1] ONU, United Nations Framework Convention for Climate Change. The Paris Agreement. http://unfccc.int/paris_agreement/items/9485.php, 2015.
[2] IRENA, Global Energy Transformation: A roadmap to 2050, in: I.R.E. Agency (Ed.) Abu Dhabi, 2018.
[3] IEA, Technology Roadmap - Hydrogen and fuel cells, Paris (France), 2015.
[4] Ghaib K, Ben-Fares FZ. Power-to-Methane: a state-of-the-art review. Renew Sustain Energy Rev 2018;81:433–46. https://doi.org/10.1016/j.rser.2017.08.004.
[5] Gur TM. Review of electrical energy storage technologies, materials and systems: challenges and prospects for large-scale grid storage. Energy Environ Sci 2018;11 (10):2696–767. https://doi.org/10.1039/c8ee01419a.
[6] Hidalgo D, Martin-Marroquin JM. Power-to-methane, coupling CO2 capture with fuel production: an overview. Renew Sustain Energy Rev 2020;132:110057. https://doi.org/10.1016/j.rser.2020.110057.
[7] Zhang XW, Chan SH, Ho HK, Tan SC, Li MY, Li GJ, et al. Towards a smart energy network: the roles of fuel/electrolysis cells and technological perspectives. Int J Hydrogen Energy 2015;40(21):6866–919. https://doi.org/10.1016/j.ijhydene.2015.03.133.
[8] Sun D, Simakov DSA. Thermal management of a Sabatier reactor for CO_2 conversion into CH4: simulation-based analysis. J CO_2 Util 2017;21:368–82. https://doi.org/10.1016/j.jcou.2017.07.015.
[9] Gotz M, Lefebvre J, Mors F, Koch AM, Graf F, Bajohr S, et al. Renewable Power-to-Gas: a technological and economic review. Renewable Energy 2016;85:1371–90. https://doi.org/10.1016/j.renene.2015.07.066.
[10] Bellotti D, Rivarolo M, Magistri L. A comparative techno-economic and sensitivity analysis of Power-to-X processes from different energy sources. Energy Convers Manage 2022;260:115565. https://doi.org/10.1016/j.enconman.2022.115565.
[11] Morgenthaler S, Ball C, Koj JC, Kuckshinrichs W, Witthaut D. Site-dependent levelized cost assessment for fully renewable Power-to-Methane systems. Energy Convers Manage 2020;223:113150. https://doi.org/10.1016/j.enconman.2020.113150.
[12] Peters R, Baltruweit M, Grube T, Samsun RC, Stolten D. A techno economic analysis of the power to gas route. J CO_2 Util 2019;34:616–34. https://doi.org/10.1016/j.jcou.2019.07.009.
[13] Baccioli A, Bargiacchi E, Barsali S, Ciambellotti A, Fioriti D, Giglioli R, et al. Cost effective power-to-X plant using carbon dioxide from a geothermal plant to increase renewable energy penetration. Energy Convers Manage 2020;226:113494. https://doi.org/10.1016/j.enconman.2020.113494.
[14] Guilera J, Morante JR, Andreu T. Economic viability of SNG production from power and CO_2. Energy Convers Manage 2018;162:218–24. https://doi.org/10.1016/j.enconman.2018.02.037.
[15] IPCC, IPCC special report on carbon dioxide capture and storage, Cambridge, UK, 2005.
[16] Adánez J, Abad A. Chemical-looping combustion: Status and research needs. Proc Combust Inst 2019;37(4):4303–17.
[17] Frigo S, Spazzafumo G. Comparison of different system layouts to generate a substitute of natural gas from biomass and electrolytic hydrogen. Int J Hydrogen Energy 2020;45(49):26166–78. https://doi.org/10.1016/j.ijhydene.2020.03.205.
[18] Bareschino P, Mancusi E, Urciuolo M, Coppola A, Solimene R, Pepe F, et al. Modelling of a combined biomass CLC combustion and renewable-energy-based methane production system for CO_2 utilization. Powder Technol 2020;373:421–32. https://doi.org/10.1016/j.powtec.2020.06.059.
[19] https://ember-climate.org/data/carbon-price-viewer/. (Accessed February 2022).
[20] E. Nieuwlaar, Life Cycle Assessment and Energy Systems Encyclopedia of Energy 2004; 3: 647-54.
[21] Abanades JC, Arias B, Lyngfelt A, Mattisson T, Wiley DE, Li H, et al. Emerging CO_2 capture systems. Int J Greenhouse Gas Control 2015;40:126–66. https://doi.org/10.1016/j.ijggc.2015.04.018.
[22] Adanez J, Abad A, Garcia-Labiano F, Gayan P, De Diego LF. Progress in chemical-looping combustion and reforming technologies. Prog Energy Combust Sci 2012;38 (2):215–82. https://doi.org/10.1016/j.pecs.2011.09.001.
[23] Mendiara T, Adánez-Rubio I, Gayán P, Abad A, De Diego LF, García-Labiano F, et al. Process comparison for biomass combustion. *in situ* gasification-chemical looping combustion (*i*G-CLC) versus chemical looping with oxygen uncoupling (CLOU). Energy Technol 4 2016:1130–6. https://doi.org/10.1002/ente.201500458.
[24] Mendiara T, García-Labiano F, Abad A, Gayán P, de Diego LF, Izquierdo MT, et al. Negative CO_2 emissions through chemical looping technology. Appl Energy 2018;232:657–84.
[25] Lyngfelt A, Leckner B. A 1000 MW_{th} boiler for chemical-looping combustion of solid fuels - Discussion of design and costs. Appl Energ 2015;157:475–87. https://doi.org/10.1016/j.apenergy.2015.04.057.
[26] Mendiara T, Gayán P, Abad A, García-Labiano F, de Diego LF, Adánez J. Characterization for disposal of Fe-based oxygen carriers from a CLC unit burning coal. Fuel Process Technol 2015;138:750–7. https://doi.org/10.1016/j.fuproc.2015.07.019.
[27] García-Labiano F, Gayán P, Adánez J, De Diego LF, Forero CR. Solid waste management of a chemical-looping combustion plant using Cu-based oxygen carriers. Environ Sci Technol 2007;41(16):5882–7. https://doi.org/10.1021/es070642n.
[28] Bareschino P, Mancusi E, Urciuolo M, Paulillo A, Chirone R, Pepe F. Life cycle assessment and feasibility analysis of a combined chemical looping combustion and power-to-methane system for CO_2 capture and utilization. Renew Sustain Energy Rev 2020;130:109962. https://doi.org/10.1016/j.rser.2020.109962.
[29] Parra D, Zhang XJ, Bauer C, Patel MK. An integrated techno-economic and life cycle environmental assessment of power-to-gas systems. Appl Energy 2017;193: 440–54. https://doi.org/10.1016/j.apenergy.2017.02.063.
[30] Blanco H, Codina V, Laurent A, Nijs W, Marechal F, Faaij A. Life cycle assessment integration into energy system models: an application for Power-to-Methane in the EU. Appl Energy 2020;259:114160. https://doi.org/10.1016/j.apenergy.2019.114160.
[31] Zhang XJ, Bauer C, Mutel CL, Volkart K. Life Cycle Assessment of Power-to-Gas: approaches, system variations and their environmental implications. Appl Energy 2017;190:326–38. https://doi.org/10.1016/j.apenergy.2016.12.098.
[32] Reiter G, Lindorfer J. Global warming potential of hydrogen and methane production from renewable electricity via power-to-gas technology. Int J Life Cycle Assess 2015;20(4):477–89. https://doi.org/10.1007/s11367-015-0848-0.
[33] Sternberg A, Bardow A. Life cycle assessment of power-to-gas: syngas vs methane. ACS Sustainable Chem Eng 2016;4(8):4156–65. https://doi.org/10.1021/acssuschemeng.6b00644.
[34] Meylan FD, Piguet FP, Erkman S. Power-to-gas through CO_2 methanation: assessment of the carbon balance regarding EU directives. J Storage Mater 2017; 11:16–24. https://doi.org/10.1016/j.est.2016.12.005.
[35] Collet P, Flottes E, Favre A, Raynal L, Pierre H, Capela S, et al. Techno-economic and Life Cycle Assessment of methane production via biogas upgrading and power to gas technology. Appl Energy 2017;192:282–95. https://doi.org/10.1016/j.apenergy.2016.08.181.
[36] [36] EC-JRC, Recommendations based on existing environmental impact assessment models and factors for life cycle assessment in the European context, ILCD Handbook. EUR24571EN. http://lct.jrc.ec.europa.eu, 2012.
[37] Sternberg A, Bardow A. Power-to-What? - Environmental assessment of energy storage systems. Energy Environ Sci 2015;8(2):389–400. https://doi.org/10.1039/c4ee03051f.
[38] Ministerio de Industria, Committee of experts on energy transition, 2017.
[39] James B, Colella W, Moton J, Saur G, Ramsden T. PEM Electrolysis H2A Production Case Study Documentation, U.S. Department of Energy, Fuel Cell Technologies Office, 2013.
[40] Muller B, Muller K, Teichmann D, Arlt W. Energy storage by CO_2 methanization and energy carrying compounds: a thermodynamic comparison. Chem Ing Tech 2011;83(11):2002–13. https://doi.org/10.1002/cite.201100113.
[41] Saidur R, Abdelaziz EA, Demirbas A, Hossain MS, Mekhilef S. A review on biomass as a fuel for boilers. Renew Sustain Energy Rev 2011;15(5):2262–89. https://doi.org/10.1016/j.rser.2011.02.015.
[42] Abad A, Adánez-Rubio I, Gayán P, García-Labiano F, de Diego LF, Adánez J. Demonstration of chemical-looping with oxygen uncoupling (CLOU) process in a 1.5 kW_{th} continuously operating unit using a Cu-based oxygen-carrier. Int J Greenh Gas Con 2012;6:189–200. https://doi.org/10.1016/j.ijggc.2011.10.016.
[43] Cabello A, Gayán P, Abad A, de Diego LF, García-Labiano F, Izquierdo MT, et al. Long-lasting Cu-based oxygen carrier material for industrial scale in Chemical Looping Combustion. Int J Greenhouse Gas Control 2016;52:120–9. https://doi.org/10.1016/j.ijggc.2016.06.023.
[44] Forero CR, Gayán P, García-Labiano F, de Diego LF, Abad A, Adánez J. High temperature behaviour of a CuO/γAl_2O_3 oxygen carrier for chemical-looping combustion. Int J Greenhouse Gas Control 2011;5(4):659–67. https://doi.org/10.1016/j.ijggc.2011.03.005.
[45] Abad A, Gayán P, García-Labiano F, de Diego LF, Adánez J. Relevance of plant design on CLC process performance using a Cu-based oxygen carrier. Fuel Process Technol 2018;171:78–88. https://doi.org/10.1016/j.fuproc.2017.09.015.
[46] Linderholm C, Schmitz M, Knutsson P, Lyngfelt A. Chemical-looping combustion in a 100-kW unit using a mixture of ilmenite and manganese ore as oxygen carrier. Fuel 2016;166:533–42. https://doi.org/10.1016/j.fuel.2015.11.015.
[47] Berguerand N, Lyngfelt A. Chemical-looping combustion of petroleum coke using ilmenite in a 10 kW_{th} unit-high-temperature operation. Energy Fuels 2009;23(10): 5257–68. https://doi.org/10.1021/ef900464j.
[48] Abad A, Adánez J, Cuadrat A, García-Labiano F, Gayán P, de Diego LF. Kinetics of redox reactions of ilmenite for chemical-looping combustion. Chem Eng Sci 2011; 66(4):689–702. https://doi.org/10.1016/j.ces.2010.11.010.
[49] Capurso T, Stefanizzi M, Torresi M, Camporeale SM. Perspective of the role of hydrogen in the 21st century energy transition. Energy Convers Manage 2022;251: 114898. https://doi.org/10.1016/j.enconman.2021.114898.

[50] Cormos CC. Chemical Looping with Oxygen Uncoupling (CLOU) concepts for high energy efficient power generation with near total fuel decarbonisation. Appl Therm Eng 2017;112:924–31. https://doi.org/10.1016/j.applthermaleng.2016.10.156.
[51] Bhave A, Taylor RHS, Fennell P, Livingston WR, Shah N, Dowell NM, et al. Screening and techno-economic assessment of biomass-based power generation with CCS technologies to meet 2050 CO_2 targets. Appl Energ 2017;190:481–9. https://doi.org/10.1016/j.apenergy.2016.12.120.
[52] Adánez J, Abad A, Mendiara T, Gayán P, de Diego LF, García-Labiano F. Chemical looping combustion of solid fuels. Prog Energy Combust Sci 2018;65:6–66. https://doi.org/10.1016/j.pecs.2017.07.005.
[53] Chauvy R, Verdonck D, Dubois L, Thomas D, De Weireld G. Techno-economic feasibility and sustainability of an integrated carbon capture and conversion process to synthetic natural gas. J CO_2 Util 2021;47:101488. https://doi.org/10.1016/j.jcou.2021.101488.
[54] Pérez-Astray A, Adánez-Rubio I, Mendiara T, Izquierdo MT, Abad A, Gayán P, et al. Comparative study of fuel-N and tar evolution in chemical looping combustion of biomass under both iG-CLC and CLOU modes. Fuel 2019;236:598–607. https://doi.org/10.1016/j.fuel.2018.09.003.
[55] Kuka E, Cirule D, Andersone I, Miklasevics Z, Andersons B. Life cycle inventory for currently produced pine roundwood. J Cleaner Prod 2019;235:613–25. https://doi.org/10.1016/j.jclepro.2019.07.004.
[56] Ecoinvent, www.ecoinvent.org, 2022.